Inorg. Chem. **2004**, *43*, 7545–7551

Chlorine Dioxide Reduction by Aqueous Iron(II) through Outer-Sphere and Inner-Sphere Electron-Transfer Pathways

Lu Wang, Ihab N. Odeh, and Dale W. Margerum*

Department of Chemistry, Purdue University, West Lafayette, Indiana 47907

Received August 27, 2004

The reduction of ClO_2 to ClO_2^- by aqueous iron(II) in 0.5 M $HClO_4$ proceeds by both outer-sphere (86%) and inner-sphere (14%) electron-transfer pathways. The second-order rate constant for the outer-sphere reaction is 1.3×10^6 M^{-1} s^{-1}. The inner-sphere electron-transfer reaction takes place via the formation of $FeClO_2^{2+}$ that is observed as an intermediate. The rate constant for the inner-sphere path (2.0×10^5 M^{-1} s^{-1}) is controlled by ClO_2 substitution of a coordinated water to give an inner-sphere complex between ClO_2 and Fe(II) that very rapidly transfers an electron to give $(Fe^{III}(ClO_2^-)(H_2O)_5^{2+})_{IS}$. The composite activation parameters for the ClO_2/$Fe(aq)^{2+}$ reaction (inner-sphere + outer-sphere) are the following: $\Delta H_r^{\ddagger} = 40$ kJ mol^{-1}; $\Delta S_r^{\ddagger} = 1.7$ J mol^{-1} K^{-1}. The $Fe^{III}ClO_2^{2+}$ inner-sphere complex dissociates to give $Fe(aq)^{3+}$ and ClO_2^- (39.3 s^{-1}). The activation parameters for the dissociation of this complex are the following: $\Delta H_d^{\ddagger} = 76$ kJ mol^{-1}; $\Delta S_d^{\ddagger} = 32$ J K^{-1} mol^{-1}. The reaction of $Fe(aq)^{2+}$ with ClO_2^- is first order in each species with a second-order rate constant of $k_{ClO_2^-} = 2.0 \times 10^3$ M^{-1} s^{-1} that is five times larger than the rate constant for the $Fe(aq)^{2+}$ reaction with $HClO_2$ in H_2SO_4 medium ($[H^+] = 0.01$–0.13 M). The composite activation parameters for the $Fe(aq)^{2+}$/Cl(III) reaction in H_2SO_4 are $\Delta H_{Cl(III)}^{\ddagger} = 41$ kJ mol^{-1} and $\Delta S_{Cl(III)}^{\ddagger} = 48$ J mol^{-1} K^{-1}.

Introduction

Chlorine dioxide has been used as an alternative disinfectant because chlorination sometimes leads to the formation of carcinogens such as trihalomethanes (THM) as well as other hazardous byproducts.[1] Chlorine dioxide is a powerful oxidant and does not form THM.[2] The disadvantage of its use in water treatment is the potential production of other undesirable disinfection byproducts such as chlorite and chlorate ions.[3,4] The disproportionation of ClO_2 forms ClO_2^- and ClO_3^- in alkaline solutions,[5−11] and its decomposition yields ClO_3^- and Cl^- in acidic solutions with exposure to sunlight.[12−15]

Little information is available about the kinetics and mechanism of the reaction between Fe^{2+} and ClO_2. Knocke and co-workers[16] reported a five-electron reduction of ClO_2 for the stoichiometry of the Fe^{2+} reaction with ClO_2 (eq 1), but they did not give a rate expression or provide sufficient information to deduce the reaction pathways. The objective of this work is to investigate the kinetics and mechanism of ClO_2 reduction by $Fe(aq)^{2+}$. To better understand the ClO_2/$Fe(aq)^{2+}$ reaction, the kinetics of the subsequent $Fe(aq)^{2+}$/Cl(III) reaction are also studied.

$$4H^+ + ClO_2 + 5Fe^{2+} \rightarrow Cl^- + 5Fe^{3+} + 2H_2O \qquad (1)$$

Experimental Section

Reagents. The method of synthesis and standardization of chlorine dioxide stock solution was described previously.[17] Solutions

* Author to whom correspondence should be addressed. E-mail: margerum@purdue.com.

(1) Rook, J. J. *J. Water Treat. Exam.* **1974**, *23*, 234−243.
(2) Lykins, B. W.; Griese, M. H. *J. Am. Water Works Assoc.* **1986**, *78*, 88−93.
(3) Werdehoff, K. S.; Singer, P. C. *J. Am. Water Works Assoc.* **1987**, *79*, 107−113.
(4) Gordon, G.; Slootmaekers, B.; Tachiyashiki, S.; Wood; D. W. *J. Am. Water Works Assoc.* **1990**, *82*, 160−165.
(5) Bray, W. C. Z. *Anorg. Allg. Chem.* **1906**, *48*, 217−250.
(6) Halperin, J.; Taube, H. *J. Am. Chem. Soc.* **1952**, *74*, 375−380.
(7) Granstrom, M. L.; Lee, G. F. *Public Works* **1957**, *88*, 90−92.
(8) Gordon, G.; Keiffer, R. G.; Rosenblatt, D. H. In *Progress in Inorganic Chemistry*; Lippard, S. J., Ed.; Wiley-Interscience: New York, 1972; pp 201−287.
(9) Emerich, D. E. Ph.D. Dissertation, Miami University, 1981.
(10) Gordon, G. *Pure Appl. Chem.* **1989**, *61*, 873−878.
(11) Odeh, I. N.; Francisco, J. S.; Margerum, D. W. *Inorg. Chem.* **2002**, *41*, 6500−6506.
(12) Basco, N.; Dogra, S. K. *Proc. R. Soc. London, Ser. A* **1971**, *323*, 29−68.
(13) Bowen E. J.; Cheung, W. M. *J. Chem. Soc.* **1932**, *159*, 1200−1207.
(14) Vel Leitner, N. K.; De Laat, J.; Dore, M. *Water Res.* **1992**, *26*, 1655−1664; **1992**, *26*, 1665−1672.
(15) Zika, R. G.; Moore, C. A.; Gidel, L. T.; Cooper, W. J. In *Water Chlorination Chemistry, Environmental Impact and Health Effect*; Lewis: Chelsea, MI, 1985; Vol. 5, pp 1041−1053.
(16) Knocke, W. R.; Van Benschoten, J. E.; Kearney, M. J.; Soborski, A. W.; Reckhow, D. A. *J. Am. Water Works Assoc.* **1991**, *83*, 80−87.

10.1021/ic048809q CCC: $27.50 © 2004 American Chemical Society
Published on Web 10/16/2004

of ClO_2 were protected from light and stored at 5 °C. The ClO_2 stock solution was standardized spectrophotometrically on the basis of the molar absorptivity of ClO_2, $\epsilon = 1230\ M^{-1}\ cm^{-1}$ at 359 nm.[17] Sodium chlorite was purified and recrystallized as described previously,[18] and stock solutions were standardized spectrophotometrically ($\epsilon = 154\ M^{-1}\ cm^{-1}$ at 260 nm).[17] Perchloric acid stock solution was prepared by dilution of Ar-sparged concentrated acid, and standardized by titration with standardized NaOH. The stock solution of Fe(II) perchlorate was prepared by dissolving reagent grade iron wire in 1 M $HClO_4$ with gentle heating to increase the rate of dissolution. The Fe^{2+} concentrations of the stock solutions were determined by titration with standardized $KMnO_4$. The $KMnO_4$ solution was standardized by the primary reagent arsenic oxide. The stock Fe^{2+} solutions for the study in H_2SO_4 medium were prepared by dissolving $Fe(NH_4)_2(SO_4)_2 \cdot 6H_2O$ in sulfuric acid. To avoid the oxidation of Fe^{2+} by oxygen dissolved in water, all Fe^{2+} solutions were made with Ar-sparged deionized, distilled water.

Kinetic Measurements. The kinetics and reaction spectra were obtained by an Applied PhotoPhysics SX 18 MV stopped-flow spectrophotometer (APPSF, optical path length = 0.962 cm). All reactions were run under pseudo-first-order conditions with $Fe(aq)^{2+}$ in large excess over $[ClO_2]$ and $[Cl(III)]_T$. Measured rate constants were corrected for mixing by accounting for the mixing rate constant.[19] Because Fe(III) readily hydrolyzes, the study was conducted in 0.50 M $HClO_4$ solution (unless otherwise specified) to prevent hydrolysis and precipitation of hydroxide species. SigmaPlot 8.0[20] was used for regression analysis.

Results and Discussion

$FeClO_2^{2+}$ Formation. Chlorine dioxide has a strong absorption band at 359 nm while $Fe(aq)^{2+}$ and $Fe(aq)^{3+}$ do not absorb significantly.[21] Nevertheless, when ClO_2 is mixed with excess $Fe(aq)^{2+}$, a first-order decay is observed at this wavelength (Figure 1a) with an average k_{obsd} value of 39.3(8) s^{-1} that is independent of the $Fe(aq)^{2+}$ concentration (Table 1). We propose that an intermediate forms rapidly and the observed absorbance decrease is due to its loss rather than the loss of ClO_2. To ascertain the existence of the intermediate, kinetic spectra are taken on the APPSF over reaction times of 20 ms (Figure 2a) and 100 ms (Figure 2b). The resulting spectra have absorbance bands from 250 to 500 nm. The absorbance in Figure 2a,b extends to higher wavelength range (>450 nm), where none of the known components ($Fe(aq)^{3+}$, $Fe(aq)^{2+}$, ClO_2, or ClO_2^-) in this system have significant absorbance. The kinetic trace taken at 500 nm (shown in Figure 3) provides evidence for the formation and decay of a new species. When $Fe(aq)^{2+}$ (0.369 mM postmixing) is mixed rapidly with ClO_2 (0.022 mM postmixing), the trace shows a fast growth in absorbance that is complete in 10 ms and is followed by a decay during the next 100 ms. The decay is first-order, and the measured rate constant is 39.3 s^{-1}. This is consistent with the first-order rate constant obtained at 359 nm (Table 1). The agreement between the first-order rate constants at 359 nm

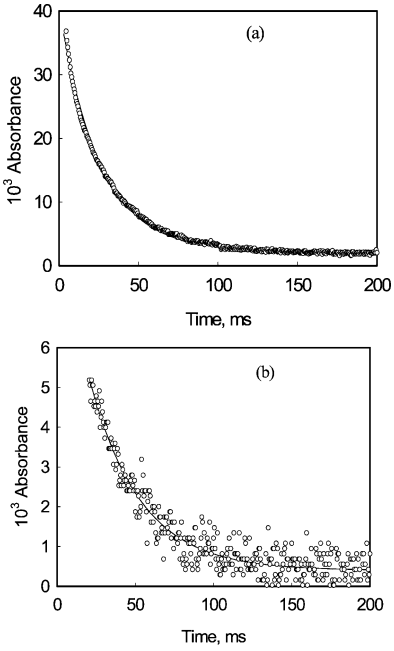

Figure 1. First-order fit kinetic traces for the decay of $FeClO_2^{2+}$: (a) λ = 359 nm; (b) λ = 500 nm. Conditions: $[Fe^{2+}] = 3.69 \times 10^{-4}$ M; $[ClO_2]_i = 2.2 \times 10^{-5}$ M; $[HClO_4] = 0.50$ M; 25.0 °C. The cell path length is 0.962 cm.

Table 1. Lack of $[Fe^{2+}]$ Dependence for the Observed Rate Constants in Studies of the ClO_2/Fe^{2+} Reaction at 359 nm in $HClO_4$[a,b]

$[Fe^{2+}]$ (mM)	k_{obsd} (s^{-1})	$[Fe^{2+}]$ (mM)	k_{obsd} (s^{-1})
2.36	40.0	1.18	38.7
1.97	39.5	0.98	38.8
1.57	38.8	0.36	40.5

[a] Conditions: $[ClO_2]_i = 9.1 \times 10^{-5}$ M, $[HClO_4] = 0.50$ M, 25.0 °C. [b] Average $k_{obsd} = 39.3(8)\ s^{-1}$.

(Figure 1a) and 500 nm (Figure 1b) indicates that the decay observed at both wavelengths can be attributed to the same intermediate species. A $FeClO_2^{2+}$ complex is the proposed intermediate formed as one of the products of the $ClO_2/Fe(aq)^{2+}$ redox reaction (eq 2). The term $FeClO_2^{2+}$ is used to represent the inner-sphere complex $(Fe^{III}(ClO_2^-)(H_2O)_5^{2+})_{IS}$.

$$Fe(aq)^{2+} + ClO_2 \rightarrow FeClO_2^{2+} \qquad K_i \qquad (2)$$

The formation of an $FeClO_2^{2+}$ complex in the Fe(III)−chlorite ion system has been reported by Fábián and Gordon.[22] They assigned the absorbance between 470 and 540 nm to $FeClO_2^{2+}$ which is consistent with our results. These authors estimated a first-order rate constant for the dissociation of $FeClO_2^{2+}$ into $Fe(aq)^{3+}$ and ClO_2 to be 19.5 s^{-1} at 25.0 °C and μ = 1.0 M ($NaClO_4$). Their observation supports our assignment of $FeClO_2^{2+}$ as the intermediate species.

Kinetics of the $ClO_2/Fe(aq)^{2+}$ Redox Reaction. The equilibrium constant for the reaction in eq 2 was reported as $K_i = 5.0 \times 10^4\ M^{-1}$.[22] The large value of K_i and our kinetic trace in Figure 3 indicate that the oxidation of $Fe(aq)^{2+}$ by ClO_2 to form $FeClO_2^{2+}$ is very favorable and rapid. Therefore, in the presence of a large excess $Fe(aq)^{2+}$,

(17) Furman, C. S.; Margerum, D. W. *Inorg. Chem.* **1998**, *37*, 4321−4327.
(18) Wang, L.; Nicoson, J. S.; Huff Hartz, K. E.; Francosco, J. S.; Margerum D. W. *Inorg. Chem.* **2002**, *41*, 108−113.
(19) Dickson, P. N.; Margerum, D. W. *Anal. Chem.* **1986**, *58*, 3153−3158.
(20) *SigmaPlot 8.0 for Windows*; SPPS Inc.: Chicago, IL, 2002.
(21) Whiteker, R. A.; Davidson, N. *J. Am. Chem. Soc.* **1953**, *75*, 3081−3085.
(22) Fábián, I.; Gordon, G. *Inorg. Chem.* **1991**, *30*, 3994−3999; **1992**, *31*, 2144−2150.

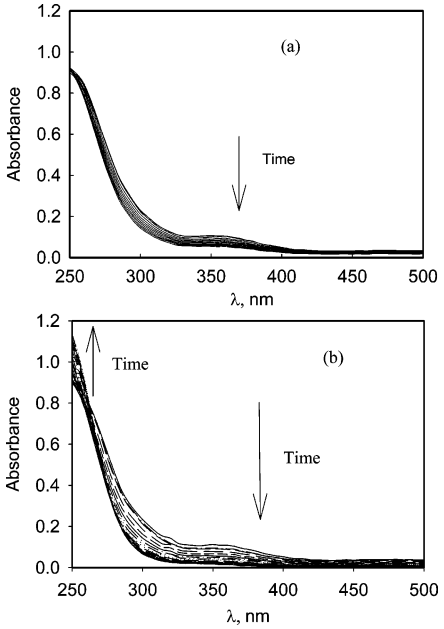

Figure 2. Kinetic spectra for the reaction of Fe^{2+} with ClO_2 in 0.50 M $HClO_4$. (a) The time interval between first scan and the last scan is 20 ms, and the time interval between scans is 0.4 ms. (b) The time interval between the first scan and the last scan is 100 ms, and the time interval between scans is 5 ms. Conditions: $[ClO_2] = 1.82 \times 10^{-4}$ M; $[Fe^{2+}] = 1.97 \times 10^{-3}$ M. The cell path length is 0.962 cm.

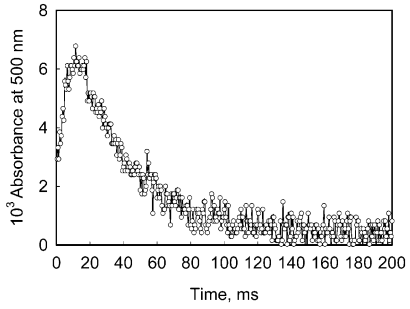

Figure 3. Kinetic profile of the Fe^{2+}/ClO_2 reaction. Conditions: $[Fe^{2+}] = 3.69 \times 10^{-4}$ M; $[ClO_2]_i = 2.2 \times 10^{-5}$ M; $[HClO_4] = 0.50$ M; 25.0 °C; $\lambda = 500$ nm. The cell path length is 0.962 cm.

the consumption of ClO_2 to produce $FeClO_2^{2+}$ is rapid. As a consequence, the decay of $FeClO_2^{2+}$ no longer depends on $[Fe^{2+}]$. The spectra in Figure 2a,b show that $FeClO_2^{2+}$ has a significant absorbance at 359 nm, where the absorbance loss of ClO_2 is compensated by the absorbance increase due to the formation of $FeClO_2^{2+}$. Since it is difficult to monitor the reaction in eq 2 at 359 nm due to the absorbance of ClO_2, the kinetics of $FeClO_2^{2+}$ formation from the Fe^{2+}/ClO_2 reaction are investigated at 500 nm. At this wavelength the absorbance of ClO_2 is negligible. A first-order reaction is observed at 500 nm (Figure 4), where the rate constant, k_{obs1}, depends on $[Fe^{2+}]$ (Figure 5). The k_{obs1} values have been corrected for the mixing efficiency of the APPSF.[19,23] From the slope of the plot in Figure 5, a second-order rate constant (k^{2nd}) of $1.5(1) \times 10^6$ M^{-1} s^{-1} is obtained for the overall reaction.

Subsequent Reaction: Cl(III)/Fe(aq)$^{2+}$. The term Cl(III) is used in the current study to represent the summation of

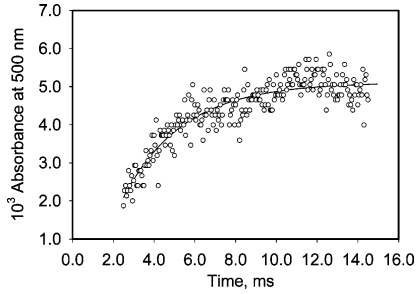

Figure 4. First-order fit of the kinetic trace for the formation of $FeClO_2^{2+}$. Conditions: $[Fe^{2+}] = 3.69 \times 10^{-4}$ M; $[ClO_2]_i = 2.2 \times 10^{-5}$ M; $[HClO_4] = 0.50$ M; 25.0 °C; $\lambda = 500$ nm. The cell path length is 0.962 cm. What is shown here is a single run.

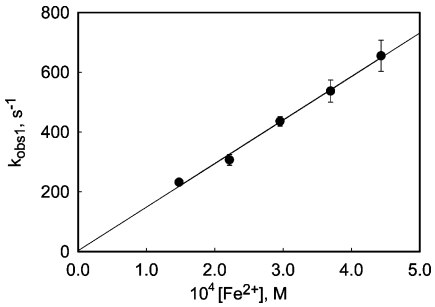

Figure 5. $[Fe^{2+}]$ dependence of the observed rate constant for the oxidation of Fe^{2+} by ClO_2. Conditions: $[ClO_2]_i = 2.2 \times 10^{-5}$ M; $[HClO_4] = 0.50$ M; 25.0 °C; $\lambda = 500$ nm; slope $= 1.5(1) \times 10^6$ M^{-1} s^{-1}; intercept $= -3(19)$ s^{-1}. Rate constants represent an average of at least five measurements at each $[Fe^{2+}]$, and standard deviations are shown. All the shown rate constants were corrected for mixing.

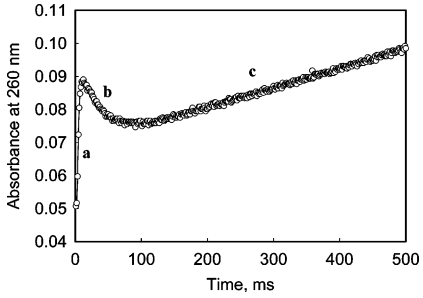

Figure 6. Kinetic profile of the Fe^{2+}/ClO_2 reaction at 260 nm: (a) formation of $[Fe(ClO_2^-)(H_2O)_5^{2+}]_{IS}$; (b) decay of $[Fe(ClO_2^-)(H_2O)_5^{2+}]_{IS}$; (c) $Fe(aq)^{3+}$ formation from Cl(III) and $Fe(aq)^{2+}$. Conditions: $[Fe^{2+}] = 3.92 \times 10^{-4}$ M; $[ClO_2]_i = 2.2 \times 10^{-5}$ M; $[HClO_4] = 0.50$ M; 25.0 °C. The cell path length is 0.962 cm.

$HClO_2$ and ClO_2^-. The kinetic spectra in Figure 2b show a growth in absorbance at 260 nm as $FeClO_2^{2+}$ decomposes. A kinetic trace at 260 nm taken over 500 ms (Figure 6) shows rapid formation of $FeClO_2^{2+}$ (Figure 6, region a) and its subsequent decay in less than 100 ms (Figure 6, region b). Another species begins to form at ~100 ms (Figure 6, region c). The kinetic trace taken at a longer reaction time under the same conditions shows a much larger absorbance increase at 260 nm within 10 s. These data fit a first-order rate constant with a $k_{obs2} = 0.39$ s^{-1} (Figure S1, Supporting Information). The reaction of $Fe(aq)^{2+}$ with Cl(III) in 2.0 M $LiClO_4/HClO_4$ has been reported.[24] The increase in absorbance in Figure 6, region c, can be assigned to the $Fe(aq)^{2+}/Cl(III)$ reaction (eq 3).

$$4Fe(II) + Cl(III) \rightarrow 4Fe(III) + Cl^- \qquad (3)$$

(23) Nicoson, J. S.; Margerum, D. W. *Inorg. Chem.* **2002**, *41*, 342−347.
(24) Ondrus, M. G.; Gordon, G. *Inorg. Chem.* **1972**, *11*, 985−989.

In our preliminary studies, H_2SO_4 was used to control the pH of the $Fe(aq)^{2+}$ reactions with ClO_2 and Cl(III). The kinetics of these reactions were followed by monitoring $FeSO_4^+$ formation at 303 nm ($\epsilon_{303} = 1960\ M^{-1}\ cm^{-1}$). The dependence of both the $Fe(aq)^{2+}/ClO_2$ and $Fe(aq)^{2+}$/Cl(III) reactions on $[Fe(aq)^{2+}]$ gave identical second-order rate constants under the same experimental conditions. On the basis of these studies, we conclude that the $Fe(aq)^{2+}/ClO_2$ reaction must be fast and the observed kinetic traces represent the subsequent $Fe(aq)^{2+}$/Cl(III) reaction. We determined the $[H^+]$ dependence of the $Fe(aq)^{2+}$/Cl(III) in H_2SO_4 medium and found that both ClO_2^- and $HClO_2$ react with $Fe(aq)^{2+}$. The pH was controlled by a HSO_4^-/SO_4^{2-} buffer, where $pK_a^{HSO_4^-} = 1.32$ at 25.0 °C and $\mu = 0.5$ M.[25] Ondrus and Gordon[24] reported that Fe(II) reacts with Cl(III) through two pathways, one with ClO_2^- and another with $HClO_2$, eq 4. We examined the same system as a part of the overall ClO_2/$Fe(aq)^{2+}$ study. Our data (Figure 7) show that the reaction of Fe^{2+} with ClO_2^- ($k_{ClO_2^-} = 2.0 \times 10^3\ M^{-1}\ s^{-1}$), eq 5a, is five times faster than the $Fe^{2+}/HClO_2$ reaction ($k_{HClO_2} = 3.5 \times 10^2\ M^{-1}\ s^{-1}$), eq 5b, where $pK_a^{HClO_2} = 1.95$ at 25.0 °C and $\mu = 0.5$ M.[26] The species Cl(II) is reduced rapidly by another $Fe(aq)^{2+}$, eq 6, to give Cl(I) (HOCl or OCl^-). HOCl reacts further with two $Fe(aq)^{2+}$ to give two $Fe(aq)^{3+}$ and Cl^-, eq 7. The findings in the literature and our preliminary results indicate that k_{HOCl} is $\sim 3.5 \times 10^3\ M^{-1}\ s^{-1}$ and is independent of the acid concentration.[27,28] Equations 8a,b are the rate expressions for the oxidation of $Fe(aq)^{2+}$ by Cl(III). The solid line in Figure 7 is a fit of the data to eq 8b.

$$HClO_2 \rightleftarrows ClO_2^- + H^+ \qquad K_a^{HClO_2} \tag{4}$$

$$Fe(aq)^{2+} + ClO_2^- \rightarrow Fe(aq)^{3+} + Cl(II) \qquad k_{ClO_2^-} \tag{5a}$$

$$Fe(aq)^{2+} + HClO_2 \rightarrow Fe(aq)^{3+} + Cl(II) + H^+ \qquad k_{HClO_2} \tag{5b}$$

$$Fe(aq)^{2+} + Cl(II) \rightarrow Fe(aq)^{3+} + Cl(I) \qquad \text{rapid} \tag{6}$$

$$2Fe(aq)^{2+} + Cl(I) \rightarrow 2Fe(aq)^{3+} + Cl^- \qquad k_{HOCl} \tag{7}$$

$$\frac{d[FeIII]}{dt} = k^{Cl(III)}[Fe(aq)^{2+}][Cl(III)] \tag{8a}$$

$$\frac{d[FeIII]}{dt} = 4\left(\frac{k_{HClO_2}[H^+] + k_{ClO_2^-}K_a^{HClO_2}}{[H^+] + K_a^{HClO_2}}\right)[Fe^{2+}][Cl(III)] \tag{8b}$$

The $[Fe^{III}SO_4]^+$ absorption band at 303 nm can be used to monitor the Fe(II) reaction with Cl(III), eqs 9 and 10. However, it is not helpful in studies of Fe(II) reaction with ClO_2 because the rate constants for the inner-sphere complexation between Fe^{3+} and SO_4^{2-}/HSO_4^- ($k^{Fe^{3+}/SO_4} = (3.5-4.6) \times 10^3\ M^{-1}\ s^{-1}$ and $k^{Fe^{3+}/HSO_4} = 51\ M^{-1}\ s^{-1}$)[29,30] are smaller than the Fe^{2+}/ClO_2 electron-transfer rate constant.

$$Fe(aq)^{3+} + SO_4^{2-} \rightarrow FeSO_4^+ \qquad k^{Fe^{3+}/SO_4} \tag{9}$$

$$Fe(aq)^{3+} + HSO_4^- \rightarrow FeSO_4^+ + H^+ \qquad k^{Fe^{3+}/HSO_4} \tag{10}$$

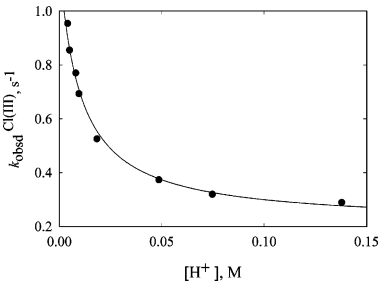

Figure 7. Dependence of the rate of Fe^{2+}/Cl(III) reaction on the acid concentration in H_2SO_4 medium. Conditions: $[Fe^{2+}] = 0.15$ mM; [Cl(III)] = 5 μM; 303 nm; 25.0 °C; $k_{HClO_2} = 3.5 \times 10^2\ M^{-1}\ s^{-1}$; $k_{ClO_2^-} = 2.0 \times 10^3\ M^{-1}\ s^{-1}$. The ionic strength at each point was controlled by the excess H_2SO_4.

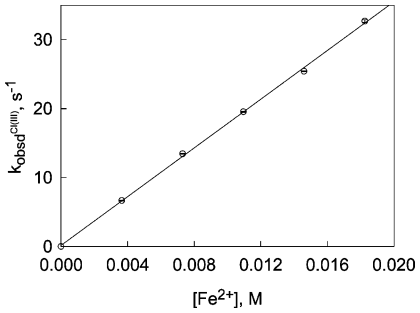

Figure 8. First-order dependence in $[Fe^{2+}]$ of the Cl(III)/$Fe(aq)^{2+}$ reaction. Conditions: $[Cl(III)]_T = 0.39$ mM; 25.0 °C; $\mu = 1.0$ M; $[HClO_4] = 0.10$ M; $\lambda = 260$ nm; slope = $1.77(2) \times 10^3\ M^{-1}\ s^{-1}$; intercept = $0.2(2)\ s^{-1}$.

We observe the kinetics of the Fe^{2+}/Cl(III) reaction in 0.11 M $HClO_4$ medium by following the first-order formation of $Fe(aq)^{3+}$ at 260 nm. The reaction has a first-order dependence in $[Fe^{2+}]$ (Figure 8) with a second-order rate constant of $1.77 \times 10^3\ M^{-1}\ s^{-1}$. This rate constant is in agreement with the value predicted in the H_2SO_4 medium on the basis of the acid-dependence study ($1.9 \times 10^3\ M^{-1}\ s^{-1}$ at $[H^+] = 0.11$ M) shown in Figure 7. This indicates that Fe^{2+}/Cl(III) reaction is not dependent on HSO_4^- and therefore data from the H_2SO_4 medium can be used to predict the rate constant for Fe^{2+}/Cl(III) reaction in the $HClO_4$ medium.

On the basis of the close values for $k^{Cl(III)}$ and k_{HOCl}, we expected complex kinetics for the Cl(III)/$Fe(aq)^{2+}$ system. Our findings included simple first-order dependence in [Cl(III)], a dependence in $[H^+]$ that follows eq 8b, and a stoichiometry of 4 for Cl(III):$Fe(aq)^{3+}$ as will be discussed later in this section. The dependence on $[H^+]$ in Figure 7 would not have been observed if HOCl/$Fe(aq)^{2+}$ was the studied reaction. Sutin and co-workers, along with our

(25) Smith, R. M.; Martell, A. E. *Critical Stability Constants. Volume 4: Inorganic Complexes*; Plenum Press: New York, 1979; p 79.
(26) Smith, R. M.; Martell, A. E. *Critical Stability Constants. Volume 4: Inorganic Complexes*; Plenum Press: New York, 1979; p 134.
(27) Conocchioli, T. J.; Hamilton, E. J.; Sutin, N. *J. Am. Chem. Soc.* **1965**, *87*, 926−927.
(28) Our preliminary data show $k_{HOCl} = 3.84(1) \times 10^3\ M^{-1}\ s^{-1}$ in 0.045 M H_2SO_4 and $3.66(3) \times 10^3\ M^{-1}\ s^{-1}$ in 0.50 M $HClO_4$.
(29) Margerum, D. W.; Cayley, G. R.; Weatherburn, D. C.; Pagenkopf, G. K. In *Coordination Chemistry*; Martell A. E., Ed.; American Chemical Society: Washington, DC, 1978; Vol. 2, p 16.
(30) Cavasino, F. P. *J. Phys. Chem.* **1968**, *72*, 1378−1384.

preliminary data, indicate that HOCl/$Fe(aq)^{2+}$ lacks dependence in acid concentration.[27,28] The experimental data enabled us to assign the observed rate constants to the Cl(III)/$Fe(aq)^{2+}$ rather than the HOCl/$Fe(aq)^{2+}$ system.

Figure 6 shows the rapid formation of a $[Fe^{III}(ClO_2^-)]^{2+}$ inner-sphere complex, region a, followed by its aquation to give $Fe(aq)^{3+}$ and Cl(III), region b. We attribute the increase in absorbance in region c of Figure 6 to the $Fe(aq)^{2+}$ reaction with Cl(III). The second-order rate constant for the observed reaction in this region is $k_{obs2}/[Fe^{2+}]' = 1.1 \times 10^3\ M^{-1}\ s^{-1}$ at 0.50 M $HClO_4$, where $[Fe^{2+}]'$ is the Fe^{2+} concentration after all the ClO_2 has reacted. This value agrees within 27% of the second-order rate constant for the Fe^{2+}/Cl(III) reaction determined on the basis of eq 8a ($1.5 \times 10^3\ M^{-1}\ s^{-1}$). The agreement suggests that the increase in absorbance at 260 nm with the first-order rate constant of k_{obs2} is due to the $Fe(aq)^{3+}$ generated from the Fe^{2+}/Cl(III) reaction. The results support the proposal that ClO_2^- is the initial product of the decay of $FeClO_2^{2+}$.

The molar absorptivity of $Fe(aq)^{3+}$, $\epsilon^{Fe^{3+}} = 2.4(1) \times 10^3\ M^{-1}\ cm^{-1}$, at 260 nm is measured in this study (Figure S2). With the value of $\epsilon^{Fe^{3+}}$ and the absorbance change ΔA (=0.221) in the reaction of Cl(III) with $Fe(aq)^{2+}$, the concentration of $Fe(aq)^{3+}$ generated is calculated to be 0.095(5) mM. Accordingly, the ratio of $[Fe(aq)^{3+}]$ formed to [Cl(III)] lost is 4.3(2), where [Cl(III)] equals the initial ClO_2 concentration (0.022 mM). This $[Fe(aq)^{3+}]$/[Cl(III)] ratio is close to the expected value of 4.0 (eq 3).

Mechanism. The reaction of ClO_2 with $Fe(aq)^{2+}$ to give ClO_2^- and $Fe(aq)^{3+}$ is thermodynamically very favorable ($K = 3700$, where K is the equilibrium constant for the oxidation of $Fe(aq)^{2+}$ by $ClO_2(aq)$ to give $Fe(aq)^{3+}$ and ClO_2^-).[31] However, two Fe^{III} products are possible. One is from an outer-sphere electron-transfer reaction to give $[Fe^{III}(H_2O)_6^{3+}]\cdot[ClO_2^-]$. In the other path ClO_2 substitution of a H_2O coordinated to Fe^{II} can give $[Fe^{II}(H_2O)_5ClO_2]_{IS}^{2+}$ followed by an extremely rapid inner-sphere electron transfer to give $[Fe^{III}(H_2O)_5ClO_2^-]_{IS}^{2+}$. The latter complex can dissociate to give $Fe^{III}(H_2O)_6^{3+}$ and ClO_2^-. In this work we can observe the formation of $[Fe^{III}(H_2O)_5ClO_2^-]_{IS}^{2+}$ due to its appreciable molar absorptivity. This enables us to separate the inner-sphere and outer-sphere pathways.

Fábián and Gordon[22] observed the formation of $FeClO_2^{2+}$ in aqueous solutions that contained $Fe(aq)^{3+}$ and ClO_2 and reported a rate constant of 269 $M^{-1}\ s^{-1}$. The rate constant determined in this study for the formation of $FeClO_2^{2+}$ from the reaction of $Fe(aq)^{2+}$ and ClO_2 is $1.5 \times 10^6\ M^{-1}\ s^{-1}$. Scheme 1 shows the various steps involved in the reduction of chlorine dioxide by $Fe(aq)^{2+}$. An electron-transfer reaction within an inner-sphere complex must be responsible for the formation of $Fe(aq)^{3+}$ and ClO_2^-. Otherwise, ClO_2^- and $Fe(aq)^{3+}$ would have been the direct products of the ClO_2/$Fe(aq)^{2+}$ reaction and no intermediate would have been observed. Therefore, the rapid formation of $FeClO_2^{2+}$ indicates an inner-sphere reaction as one of the electron-transfer pathways. However, electron transfer via an outer-sphere reaction is also possible.

Table 2. Evidence for Outer-Sphere and Inner-Sphere Electron-Transfer Reactions of $Fe(aq)^{2+}$ with ClO_2[a]

$10^4[ClO_2]_i$ (M)	$10^4[FeClO_2^{2+}]_{IS}$ (M)[b]	A_{calc}[c]	A_{meas}[d]	% inner sphere[e]
2.05	1.84	0.113	0.013	14
2.56	2.22	0.136	0.016	14

[a] Conditions: $[Fe^{2+}] = 3.58 \times 10^{-4}$ M, $[HClO_4] = 0.50$ M, 25.0 °C. [b] $[FeClO_2^{2+}]$ is calculated from $K_i = 5.0 \times 10^4\ M^{-1}$,[22] $[ClO_2]_i$, and $[Fe^{2+}]$. [c] A_{cal} is calculated from the $\epsilon_{510} = 636 \pm 10\ M^{-1}\ cm^{-1}$ [22] and the $[FeClO_2^{2+}]$ assuming 100% inner-sphere electron transfer. [d] A_{meas} is measured for the reaction of Fe(II) and ClO_2 at 510 nm. [e] $100A_{meas}/A_{calc}$ after A_{meas} was corrected to account for the overlap between $FeClO_2^{2+}$ formation and decay as shown in eqs 11 and 12. The k_i and k_d values are $1.8 \times 10^5\ M^{-1}\ s^{-1}$ (based on 12%) and 39.3 s^{-1}, respectively.

Scheme 1. Mechanism for Chlorine Dioxide Reduction by $Fe(aq)^{2+}$ via Outer-Sphere and Inner-Sphere Pathways and $Fe(aq)^{3+}$ Complexation with Chlorite Ion

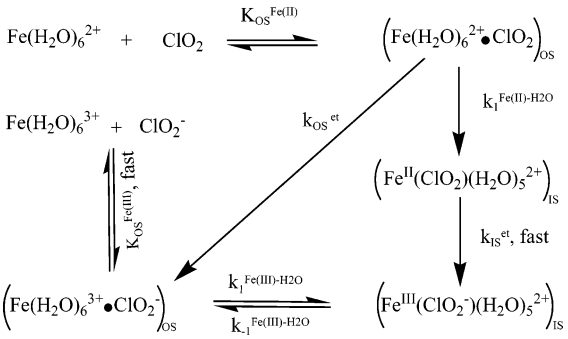

The reported molar absorptivity for $FeClO_2^{2+}$ is $\epsilon_{510} = 636(10)\ M^{-1}\ cm^{-1}$.[22] By use of this molar absorptivity, we can determine whether ClO_2 reacts only by inner-sphere electron transfer or if it reacts by a mixture of inner-sphere and outer-sphere paths. To enhance the signal at 510 nm, higher $[ClO_2]$ (0.205 and 0.256 mM) are used to react with a slight excess Fe^{2+} (0.358 mM) so that the reaction is not too fast to measure on the APPSF. Due to the deadtime of the stopped-flow instrument (~2.5 ms), extrapolation to zero time after correcting for mixing was needed. Table 2 summarizes the results. The A_{meas} is the maximum absorbance of $FeClO_2^{2+}$ measured at 510 nm for five kinetic traces. A_{calc} is the value of absorbance calculated from $\epsilon = 636\ M^{-1}\ cm^{-1}$ and $[FeClO_2^{2+}]$ (where $[FeClO_2^{2+}]$ is the equilibrium concentration calculated from $K_i = 5.0 \times 10^4\ M^{-1}$,[22] $[ClO_2]_i$, and $[Fe^{2+}]$). A comparison of A_{meas} and A_{calc} values indicates that only 12% of $[ClO_2]_i$ reacts with $Fe(aq)^{2+}$ via an inner-sphere path. The other 88% of $[ClO_2]_i$ must react by an outer-sphere path.

However, because of the overlap between the formation and decay reactions of the intermediate (seen in parts a and b of Figure 6 at 260 nm), the true maximum absorbance of $FeClO_2^{2+}$ is greater than that observed and reported in Table 2 at 510 nm. In the kinetic study, where $[Fe(aq)^{2+}]$ is present at much higher levels than $[ClO_2]$, we can predict the maximum $[FeClO_2^{2+}]$ by use of eqs 11 and 12.[32]

In eq 12, k_i is the rate constant for $FeClO_2^{2+}$ formation and k_d is the rate constant for its decay (39.3 s^{-1}). The

(31) Schmitz, G.; Rooze, H. *Can. J. Chem.* **1984**, *62*, 2231−2234; **1985**, *63*, 975−980.

(32) Espenson, J. H. *Chemical Kinetics and Reaction Mechanisms*, 2nd ed.; McGraw-Hill: New York, 1995; p 71.

significance of k_i is discussed further in the following section. Equation 12 permits us to predict that the inner-sphere path is 14% of the overall reaction (rather than 12%). This value was obtained on the basis of an iteration by use of the conditions in Figure 4 at 500 nm ($[Fe(aq)^{2+}] = 3.69 \times 10^{-4}$ M, $[ClO_2] = 2.2 \times 10^{-5}$ M, $FeClO_2^{2+}$ $\epsilon_{500} = 600$ M^{-1} cm^{-1}, observed $A_{max} = 0.005$, $k_d = 39.3$ s^{-1}, and initial $k_i = 1.8 \times 10^5$ M^{-1} s^{-1}). Hence the outer-sphere electron-transfer path represents 86% (rather than 88%) after correction for this overlap.

$$Fe(aq)^{2+} + ClO_2 \xrightarrow{k_i} FeClO_2^{2+} \xrightarrow{k_d} Fe(aq)^{3+} + ClO_2^- \quad (11)$$

$$[FeClO_2^{2+}] = [ClO_2]\left(\frac{k_d}{[Fe(aq)^{2+}]k_i}\right) \exp\left(\frac{k_d}{[Fe(aq)^{2+}]k_i - k_d}\right) \quad (12)$$

Note that the literature value for the equilibrium constant K_i was determined by the use of much higher initial concentrations of $Fe(aq)^{3+}$ and ClO_2^-.[22] The accuracy of the percent contribution from each of the pathways is based on the literature molar absorptivity and equilibrium constant.[22]

Resolution of Rate Constants. Although the second-order rate constant, $k^{2nd} = 1.5 \times 10^6$ M^{-1} s^{-1}, is obtained by following the formation of $FeClO_2^{2+}$, it reflects the loss of ClO_2 by all the reactions that consume it. Therefore, the k^{2nd} value is actually a summation of the inner-sphere path ($k_i = K_{OS}^{Fe(II)} k_1^{Fe(II)-H_2O}$) and the outer-sphere path ($k_o = K_{OS}^{Fe(II)} k_{OS}^{et}$). The inner-sphere rate constant $k_i = 2.0(1) \times 10^5$ M^{-1} s^{-1} is obtained by eq 13. The α term is the fractional contribution of the inner-sphere path (14%). From the k_i and k^{2nd} values, the second-order rate constant for the outer-sphere path is $1.3(1) \times 10^6$ M^{-1} s^{-1}.[33]

$$k_i = \alpha k^{2nd} \quad (13)$$

The $Fe^{2+}-H_2O$ exchange rate constant ($k_1^{Fe(II)-H_2O}$) is 3.2×10^6 s^{-1}, and Fe^{2+} is expected to have a $K_{OS}^{Fe(II)}$ with a value of 0.1 for the neutral ligand.[34] Hence, the substitution rate constant ($K_{OS}^{Fe(II)}$ $k_1^{Fe(II)-H_2O}$) is estimated to be 3×10^5 M^{-1} s^{-1}, which is in reasonable agreement with the measured k_i value (2.0×10^5 M^{-1} s^{-1}). This indicates that the substitution step ($k_1^{Fe(II)-H_2O}$) is the rate-determining step in the inner-sphere path and is followed by a fast electron transfer (k_{IS}^{et}) to form $FeClO_2^{2+}$. The outer-sphere electron transfer occurs with a second-order rate constant $k_o = 1.3 \times 10^6$ M^{-1} s^{-1}.

By using the corresponding standard electrode potentials, Schmitz and Rooze[31] estimated the equilibrium constant for the reduction of ClO_2 to ClO_2^- by Fe^{2+} in 1.0 M $NaClO_4$ at 25 °C: $K = [ClO_2^-][Fe^{3+}]/([ClO_2][Fe^{2+}]) = 3.7 \times 10^3$. From this K value and the self-exchange rate constant values of $k_{ClO_2/ClO_2^-} = 2.0 \times 10^2$ M^{-1} s^{-1} [35] and $k_{Fe^{2+}/Fe^{3+}} = 5.6$ (0.5 M $NaClO_4$, 25.0 °C),[36] the rate constant for the outer-sphere electron transfer is estimated to be 1.7×10^3 M^{-1} s^{-1} on the basis of Marcus theory.[37] The measured rate constant (1.3×10^6 M^{-1} s^{-1}) for the outer-sphere path is 765 times larger than expected by simplified Marcus theory. Deviation from the simplified Marcus theory may occur in the case of small molecules,[38] where orbital overlap occurs.

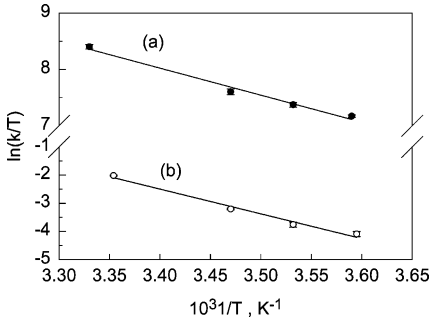

Figure 9. Eyring plots. (a) The electron-transfer reaction between ClO_2 and $Fe(aq)^{2+}$ by outer-sphere and inner-sphere paths. Slope = $-4.8(4) \times 10^3$, and intercept = 24(2). (b) The dissociation of $FeClO_2^{2+}$ into ClO_2^- and $Fe(aq)^{3+}$. Slope = $-8.8(7) \times 10^3$, and intercept = 27(3). Conditions: $[Fe^{2+}] = 0.392$ mM; $[ClO_2]_i = 0.040$ mM; $[HClO_4] = 0.50$ M; temperature range 5.0−25.0 °C; $\lambda = 500$ nm.

Fábián and Gordon[22] predicted the second-order rate constant for the reaction in eq 2 to have a value of 1.5×10^6 M^{-1} s^{-1} (pH 1.0−3.5, $\mu = 1.0$ M, and 25 °C) on the basis of their calculated equilibrium constant for eq 2 and the measured rate constant values for the $Fe(aq)^{3+}/ClO_2^-$ reaction ($K_{OS}^{Fe(III)} k_{-1}^{Fe(III)-H_2O}$). This agrees with our experimental results. However, they were not able to distinguish the inner-sphere and outer-sphere paths for the $ClO_2/Fe(aq)^{2+}$ reaction in their studies. The current study shows that the $Fe(aq)^{2+}$ reaction with ClO_2 is 500 times faster than what was reported by Hoigné and Bader ($k_{rxn} = 3.0(5) \times 10^3$ M^{-1} s^{-1}),[39] who could have been misled by the decay profile of the subsequent reaction of ClO_2^- with $Fe(aq)^{2+}$.

Activation Parameters. The activation parameters for the reduction of ClO_2 by $Fe(aq)^{2+}$ and the $FeClO_2^{2+}$ decay are determined from the temperature dependence of the rates in 0.50 M perchloric acid. The Eyring plot in Figure 9a yields values of $\Delta H_r^{\ddagger} = 40(5)$ kJ mol^{-1} and $\Delta S_r^{\ddagger} = 1.7(2)$ J mol^{-1} K^{-1} for the reaction of ClO_2 with $Fe(aq)^{2+}$. Because the k^{2nd} value represents both inner-sphere and outer-sphere paths, the $\Delta H_r^{\ddagger}$ and the $\Delta S_r^{\ddagger}$ obtained from the measurement of the k^{2nd} values are composite parameters. The outer-sphere path (86%) dominates the reaction, so the values of $\Delta H_r^{\ddagger}$

(33) k^{2nd} is the overall second-order rate constant. $k_i = K_{OS}^{Fe(II)} k_1^{Fe(II)-H_2O}$ and $k_o = K_{OS}^{Fe(II)} k_{OS}^{et}$ are the second-order inner-sphere and outer-sphere rate constants for the pathways of the $Fe(aq)^{2+}/ClO_2$ reaction, respectively. $K_{OS}^{Fe(II)}$ is the equilibrium constant to form $(Fe(H_2O)_6^{2+} \cdot ClO_2)_{IS}$, $k_1^{Fe(II)-H_2O}$ is the water-exchange constant for Fe(II), and k_{OS}^{et} is the electron-transfer rate constant for the outer-sphere pathway.

(34) Margerum, D. W.; Cayley, G. R.; Weatherburn, D. C.; Pagenkopf, G. K. In *Coordination Chemistry*; Martell A. E., Ed.; American Chemical Society: Washington, DC, 1978; Vol. 2, pp 12−13.

(35) Stanbury, D. M. *Advances in Chemistry Series: Electron-Transfer Reactions*; American Chemistry Society: Washington, DC, 1997; pp 165−182.

(36) (a) Lappin, G. In *Redox Mechanisms in Inorganic Chemistry*; Burgess, J., Ed.; Ellis Horwood Series in Inorganic Chemistry; Ellis Horwood: Chichester, U.K., 1994; p 60. (b) Jolley, W. H.; Stranks, D. R.; Swaddle, T. W. *Inorg. Chem.* **1990**, *29*, 1948−1951. (c) Brunschwig, B. S.; Creutz, C.; Macartney, D. H.; Sham, T.-K.; Sutin, N. *Faraday Discuss. Chem. Soc.* **1982**, *74*, 113−127.

(37) Espenson, J. H. *Chemical Kinetics and Reaction Mechanisms*, 2nd ed.; McGraw-Hill: New York, 1995; pp 243−247.

(38) Awad, H. H.; Stanbury, D. M. *J. Am. Chem. Soc.* **1993**, *115*, 3636−3642.

(39) Hoigné, J.; Bader, H. *Water Res.* **1994**, *28*, 45−55.

Table 3. Summary of the Rate Constants and the Activation Parameters

reaction	rate const[a]	$\Delta H^{\ddagger}$ (kJ mol^{-1})	$\Delta S^{\ddagger}$ (J mol^{-1} K^{-1})
$ClO_2 + Fe(aq)^{2+} \rightarrow ClO_2^- + Fe(aq)^{3+}$	1.3×10^6 M^{-1} s^{-1} [b,c]	40(5)[e,f]	1.7(2)[e,f]
$ClO_2 + Fe(aq)^{2+} \rightarrow FeClO_2^{2+}$	2.0×10^5 M^{-1} s^{-1} [b,d]		
$FeClO_2^{2+} \rightarrow Fe(aq)^{3+} + ClO_2^-$	39.3 s^{-1} [b]	76(9)[e,f]	32(5)[e,f]
$HClO_2 + Fe(aq)^{2+} \rightarrow Cl(II) + Fe(aq)^{3+} + H^+$	3.5×10^2 M^{-1} s^{-1} [g]	41(1)[h,i]	48(1)[h,i]
$ClO_2^- + Fe(aq)^{2+} \rightarrow Cl(II) + Fe(aq)^{3+}$	2.0×10^3 M^{-1} s^{-1} [g]		

[a] Conditions: 25.0 °C. [b] Conditions: $[HClO_4] = 0.50$ M. [c] Outer-sphere pathway for the $ClO_2/Fe(aq)^{2+}$ reaction (k_o). [d] Inner-sphere pathway for the $ClO_2/Fe(aq)^{2+}$ reaction (k_i). [e] Temperature range 5.0−25.0 °C, $[HClO_4] = 0.50$ M. [f] The values are for a combination of inner-sphere and outer-sphere paths. [g] Conditions: 0.01−0.14 M $[H^+]$ in H_2SO_4 medium. The initial product, Cl(II), reacts further with another $Fe(aq)^{2+}$ to give HOCl. HOCl is reduced by $2Fe(aq)^{2+}$ to Cl^-. [h] These are composite values for the reactions of both forms of Cl(III) with $Fe(aq)^{2+}$ in 0.4 M $[H^+]$ and μ adjusted to 1.0 M by Na_2SO_4. Temperature range = 20−40 °C. [i] $\Delta H_{HClO_2}^{\circ} = 17.2$ kJ mol^{-1}.

and $\Delta S_r^{\ddagger}$ reflect the features of the outer-sphere path more than those of the inner-sphere path. The Eyring plot in Figure 9b yields values of $\Delta H_d^{\ddagger} = 76(9)$ kJ mol^{-1} and $\Delta S_d^{\ddagger} = 32(5)$ J K^{-1} mol^{-1} for the decomposition of $FeClO_2^{2+}$ to generate $Fe(aq)^{3+}$ and ClO_2. The Eyring plot for $Fe(aq)^{2+}/Cl(III)$ reaction ($[H^+] = 0.40$ M and $\mu = 1.0$ M (Na_2SO_4)) leads to the composite activation parameters $\Delta H_{Cl(III)}^{\ddagger} = 41(1)$ kJ mol^{-1} and $\Delta S_{Cl(III)}^{\ddagger} = 48(1)$ J K^{-1} mol^{-1} (temperature range = 20−40 °C) as shown in Figure S3. These composite activation paramters represent the effect of temperature on the rate constants for both $Fe(aq)^{2+}/ClO_2^-$ and $Fe(aq)^{2+}/HClO_2$ reactions as well as on the $K_a^{HClO_2}$ values. The enthalpy for the protonation constant of $HClO_2$ is 17.2 kJ mol^{-1} (10−60 °C).[26] At 25.0 °C, the ratio of $[HClO_2]/[ClO_2^-]$ is 35.5 in 0.4 M acid and the $k_{HClO_2}/k_{ClO_2^-}$ ratio is 0.18. At 40.0 °C the $[HClO_2]/[ClO_2^-]$ ratio increases to 50. Although the composite activation parameters are not resolved for the $Fe(aq)^{2+}$ reactions with $HClO_2$ and ClO_2^-, the dominant reaction is with $HClO_2$ at the acidities used. Therefore, these activation parameters should correspond approximately to those for the $HClO_2$ reaction. Table 3 is a summary of all the rate constants and activation parameters obtained in this study. Confidence intervals for the activation parameters were calculated on the basis of a *t*-value of 2.92 at the 90% level.[40]

Acknowledgment. This work was supported by National Science Foundation Grants CHE-9818214 and CHE-0139876. We thank Deedra Pell (a freshman honor student) for her measurement of the molar absorptivity of $FeSO_4^+$.

Supporting Information Available: Figures with supplemental data. This material is available free of charge via the Internet at http://pubs.acs.org.

IC048809Q

(40) Skoog, D. A.; West, D. M.; Holler, F. J. *Fundamentals of Analytical Chemistry*, 7th ed.; Saunders College: Orlando, FL, 1997; pp 48−50.